# Regulation of *Drosophila* courtship behavior by the *Tlx/tailless*-like nuclear receptor, *dissatisfaction*

### **Highlights**

- dsf is expressed in neurons broadly distributed across the female and male CNSs
- dsf and dsx neurons contribute to sex-specific abdominal courtship behaviors
- dsf acts oppositely in females and males depending upon male-specific dsx

### **Authors**

Julia C. Duckhorn, Jessica Cande, Mary C. Metkus, Hyeop Song, Sofia Altamirano, David L. Stern, Troy R. Shirangi

### Correspondence

troy.shirangi@villanova.edu

### In brief

Duckhorn et al. identify a group of sexually dimorphic dissatisfaction-expressing interneurons that contribute to female- and male-specific abdominal courtship behaviors. dissatisfaction acts as a pro- or anti-female factor for the development and function of these neurons depending upon the sexual state of doublesex expression.





### **Article**

# Regulation of *Drosophila* courtship behavior by the *Tlx/tailless-like* nuclear receptor, *dissatisfaction*

Julia C. Duckhorn, <sup>1</sup> Jessica Cande, <sup>2</sup> Mary C. Metkus, <sup>1</sup> Hyeop Song, <sup>1</sup> Sofia Altamirano, <sup>1</sup> David L. Stern, <sup>2</sup> and Troy R. Shirangi<sup>1,3,\*</sup>

<sup>1</sup>Villanova University, Department of Biology, 800 East Lancaster Ave, Villanova, PA 19085, USA

<sup>2</sup> Janelia Research Campus, Howard Hughes Medical Institute, 19700 Helix Drive, Ashburn, VA 20147, USA

<sup>3</sup>Lead contact

\*Correspondence: troy.shirangi@villanova.edu https://doi.org/10.1016/j.cub.2022.02.031

### **SUMMARY**

Sexually dimorphic courtship behaviors in *Drosophila melanogaster* develop from the activity of the sexual differentiation genes, *doublesex* (*dsx*) and *fruitless* (*fru*), functioning with other regulatory factors that have received little attention. The *dissatisfaction* (*dsf*) gene encodes an orphan nuclear receptor homologous to vertebrate *Tlx* and *Drosophila tailless* that is critical for the development of several aspects of female- and male-specific sexual behaviors. Here, we report the pattern of *dsf* expression in the central nervous system and show that the activity of sexually dimorphic abdominal interneurons that co-express *dsf* and *dsx* is necessary and sufficient for vaginal plate opening in virgin females, ovipositor extrusion in mated females, and abdominal curling in males during courtship. We find that *dsf* activity results in different neuroanatomical outcomes in females and males, promoting and suppressing, respectively, female development and function of these neurons depending upon the sexual state of *dsx* expression. We posit that *dsf* and *dsx* interact to specify sex differences in the neural circuitry for dimorphic abdominal behaviors.

### **INTRODUCTION**

The neural circuitry for sex-specific behaviors in *Drosophila melanogaster* is currently understood to be specified during development by transcriptional regulators encoded by the *doublesex* (*dsx*) and *fruitless* (*fru*) genes. The male isoforms of *dsx* and *fru* direct the differentiation of neurons in the adult male CNS that are required for performance of male courtship behaviors. Conversely, the female-specific isoform of the *dsx* gene together with the absence of male-specific *fru* build the neural pathways that direct female-specific sexual behaviors. 3,6-9

Although dsx and fru are indispensable for sexual differentiation of the Drosophila nervous system, they act together with other regulatory genes that have been less well studied. 10,11 The dissatisfaction (dsf) gene, for instance, which encodes an orphan nuclear receptor homologous to vertebrate Tlx and Drosophila tailless, is required for several aspects of femaleand male-specific reproductive behaviors. 12,13 Females that are homozygous for null mutations of dsf rarely mate with courting males and, if fertilized, are unable to lay eggs despite being able to ovulate. 12 Males mutant for dsf court females and males indiscriminately and are delayed in copulating with females at least in part due to deficits in abdominal bending during copulation attempts. 12 The dsf gene was first identified over 20 years ago, yet where and when dsf is precisely expressed in the Drosophila nervous system, which dsf-expressing neurons matter for courtship behavior, and how dsf contributes to the sexual differentiation of the nervous system are not known.

Here, we report dsf's spatial and temporal expression in the CNS and discover a small group of sexually dimorphic dsf and dsx co-expressing interneurons in the abdominal ganglion called the dsf-dsx abdominal ganglion (DDAG) neurons. Females and males have ~11 and 3 DDAG neurons per side, respectively, that exhibit sexually dimorphic projection patterns in the ventral nerve cord (VNC). Optogenetic activation and neural silencing experiments demonstrate that the DDAG neurons contribute to vaginal plate opening in virgin females, ovipositor extrusion in mated females, and abdominal curling in males during courtship. dsf promotes the presence of female-specific DDAG neurons and the development of vaginal plate opening behavior in virgin females. In males, dsf acts in an opposite manner, suppressing the development of a single female-like DDAG neuron. Optogenetic activation of artificially induced female-like DDAG neurons in males drives an abdominal behavior in males that imitates vaginal plate opening or ovipositor extrusion in females. We show that dsf promotes or suppresses female-like development and function of the DDAG neurons depending upon the expression of the male isoform of dsx. Taken together, our results reveal new insights into the dsf gene and its regulation of neurodevelopment and sex-specific abdominal behaviors.

### **RESULTS**

### Expression of dsf in the Drosophila CNS

In a previous study, <sup>13</sup> dsf expression in the *Drosophila* CNS was detected by *in situ* hybridization in a small number of neurons



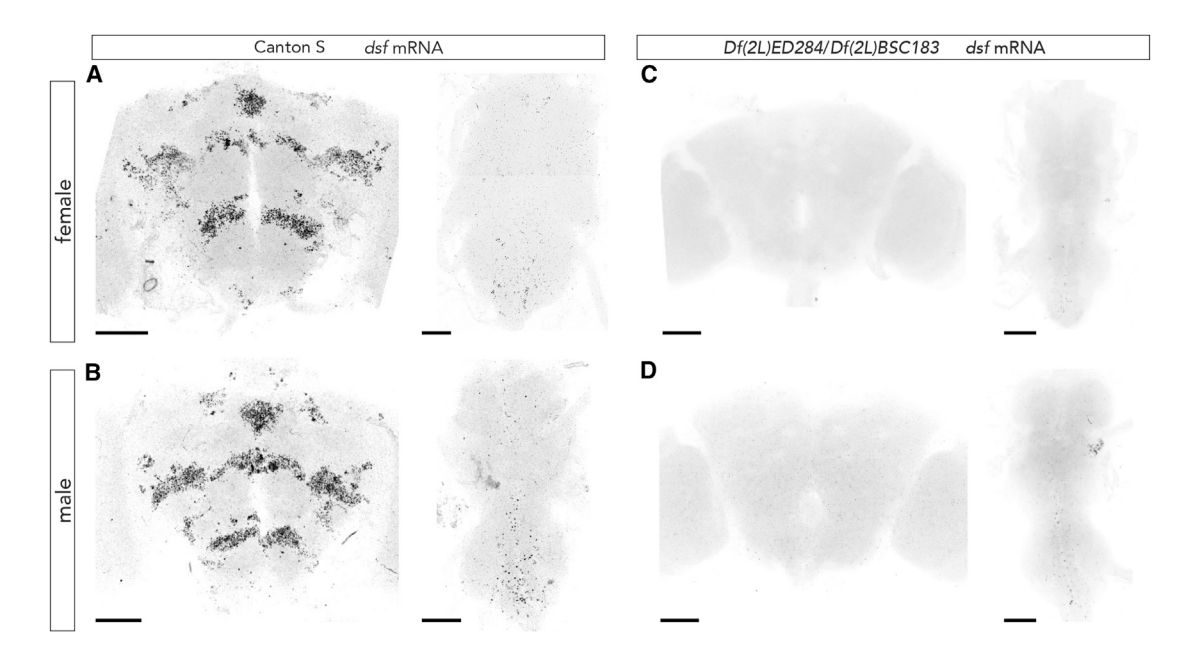


Figure 1. Expression of dsf mRNA in the adult Drosophila CNS (A-D) Confocal image of an adult Canton S female (A) and male (B) brain and VNC showing dsf mRNA expression labeled by in situ HCR using a probe-set directed against dsf transcripts. Hybridization signals are seen in several groups of cells in the brain and VNC. dsf mRNA expression was not detected in the CNSs of females (C) and males (D) carrying partially overlapping deficiencies that delete the dsf gene. Scale bars represent 50 µm.

located primarily in anterior regions of the pupal and adult protocerebrum. We reexamined dsf mRNA expression in the adult CNS by in situ hybridization chain reaction (HCR), a robust, quantitative, and sensitive method to detect mRNAs in wholemounted tissues. 14-17 Using HCR probe-sets directed against dsf, we observed dsf mRNAs in the Canton S CNS in substantially more cells than originally reported (Figures 1A and 1B). In the brain, dsf expression was found in several broadly distributed clusters of cells located mostly on the anterior side, dorsal and ventral to the foramen of the esophagus. Hybridization signals were also detected in a few cells in the thoracic and abdominal neuromeres of the VNC. The intensities and distributions of hybridization signals appeared similar between the sexes, and hybridization signals were not detected in flies that are null for the dsf gene (Figures 1C and 1D).

To characterize the identity, anatomy, and function of dsf-expressing cells, we used CRISPR/Cas9-mediated homologydirected repair to insert the Gal4 transcriptional activator from yeast into the dsf translational start codon, generating a dsf Gal4 allele (Figure 2A). Insertion of Gal4 deleted all coding sequences within dsf's first exon and the exon's 5' splice site, thereby creating a loss-of-function allele. We assessed whether  $\textit{dsf}^{\text{Gal4}}$ reproduces the endogenous pattern of dsf transcripts by sequentially applying in situ HCR and immunohistochemistry to adult CNS tissues from flies heterozygous for dsf<sup>Gal4</sup> and carrying UAS-nls::gfp to simultaneously detect dsf transcripts and GFP expression. We found an almost perfect overlap of the two markers in the adult brain and VNC of females and males (Figures 2B and 2C). All cells in the adult CNS labeled by dsf<sup>Gal4</sup> co-expressed the pan-neuronal marker encoded by the embryonic lethal abnormal vision gene, elav, confirming that the dsf-expressing cells are neuronal (Figures S1A–S1D).

We categorized dsf-expressing neurons as belonging to specific clusters of neurons and used standardized nomenclature 18,19 to assign names to each neuronal group based on their location in the cell body rind of the brain and VNC (Figures 2D-2F). dsf-expressing neurons in the brain occur in 12 discernible groups on the left and right sides. Eight of the neuronal groups are in the supraesophageal zone of the brain and four are present in the subesophageal zone. All 12 groups of neurons are present in both sexes, but some groups (i.e., rSMPma, rALad, and rALv) exhibit notable differences in neuron number between the sexes (Figure 2F). Additionally, females have a greater number of dsfexpressing neurons than males in the abdominal ganglion of the VNC (Figure 2F).

When driving a membrane-targeted GFP, dsf<sup>Gal4</sup> labeled many different nerve bundles and synaptic neuropils present mostly on the posterior side of the adult brain and in the VNC (Figures 2G and 2H). No obvious sex differences in the projection patterns of dsf-expressing neurons were observed in the adult CNS. dsf<sup>Gal4</sup> also labeled subsets of neurons in the late 3<sup>rd</sup> instar larval and pupal (Figures S1E-S1J) CNS.

dsf mutant females and males were reported to display abnormalities in motoneuron innervation on muscles of the uterus and ventral abdomen, respectively. 12 We did not detect dsf Gal4 activity in motoneurons (or peripheral sensory neurons) at any stage that we examined, nor in muscles of the ventral abdomen or uterus. To further confirm that dsfGal4 accurately labeled all dsf-expressing neurons in the abdominal ganglion, we sequentially detected dsf mRNAs and GFP and ELAV protein expression in CNS tissue from dsf<sup>Gal4</sup> > myr::gfp flies. dsf hybridization signals were detected exclusively in ELAV-expressing neurons that co-expressed GFP, indicating that all dsf-expressing neurons are targeted by the dsf<sup>Gal4</sup> allele (Figure S1K). These data





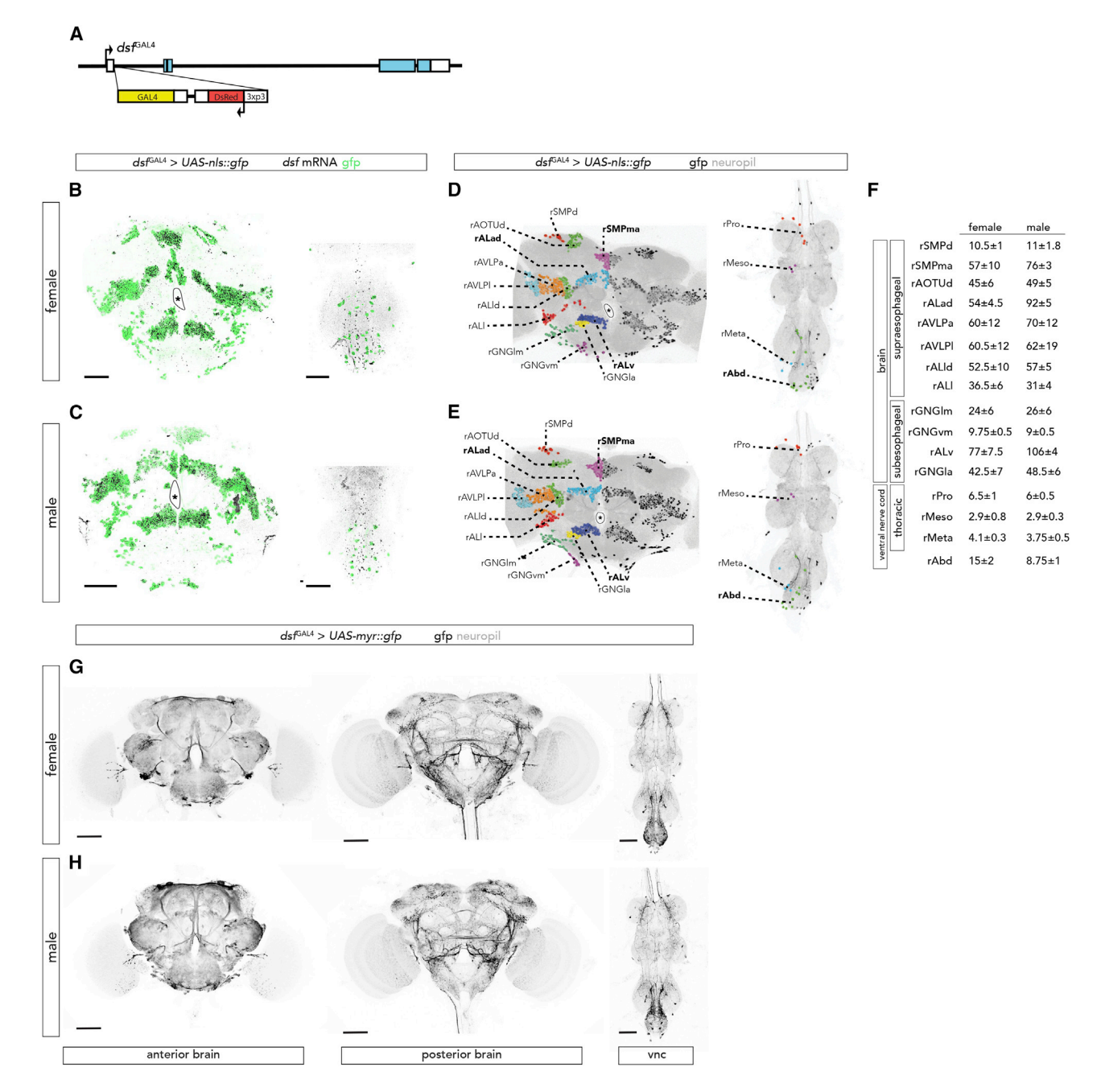


Figure 2. dsf<sup>Gal4</sup> labels dsf-expressing neurons in the female and male adult CNS

(A) Design of the dsf<sup>Gal4</sup> allele. Targeted insertion of the Gal4 coding sequence (yellow box) after dsf's translational start codon in exon 1 allows expression of Gal4 wherever dsf is normally expressed. Each box represents an exon. Exonic regions colored in light blue and white represent dsf coding sequences and untranslated regions, respectively.

(B and C) Confocal images of the adult brain and third thoracic and abdominal ganglia of the VNC from dsf<sup>Gal4</sup> > UAS-nls::gfp females (B) and males (C) showing colocalization of dsf mRNA (black) and GFP protein (green) labeled by combined in situ HCR and immunohistochemistry. dsf mRNA and GFP protein expression overlap in the brain. GFP-expressing cells in the VNC exhibit in situ HCR signals; however, some hybridization signals in the VNC lack GFP expression. These hybridization signals are non-specific to dsf as they persist in the VNCs of flies carrying deficiencies that delete the dsf locus (see Figures 1C and 1D). Scale bars represent 50 µm. (D and E) Confocal images of brains and VNCs from  $dsf^{Sal4} > UAS-nls.::gfp$  females (D) and males (E) showing the distribution of GFP-expressing neurons in black and DNCad (neuropil) in light gray. Discrete groups of neurons were color-coded and categorized on one side of the brain according to standardized nomenclatures. Neuronal groups that exhibit sex differences in neuron number are labeled in bold. See also Figure S1.

(F) Table showing the average number (± standard deviation [SD]) of neurons in each dsf<sup>Gal4</sup>-expressing neuronal group (N = 4 sides/group) in the brain and VNC

(G and H) Confocal images of brains and VNCs from dsf Gal4 > UAS-myr::gfp of females (G) and males (H) showing the projection and arborization patterns of dsf<sup>Gal4</sup>-expressing neurons in black and DNCad (neuropil) in light gray. Scale bars represent 50 μm.



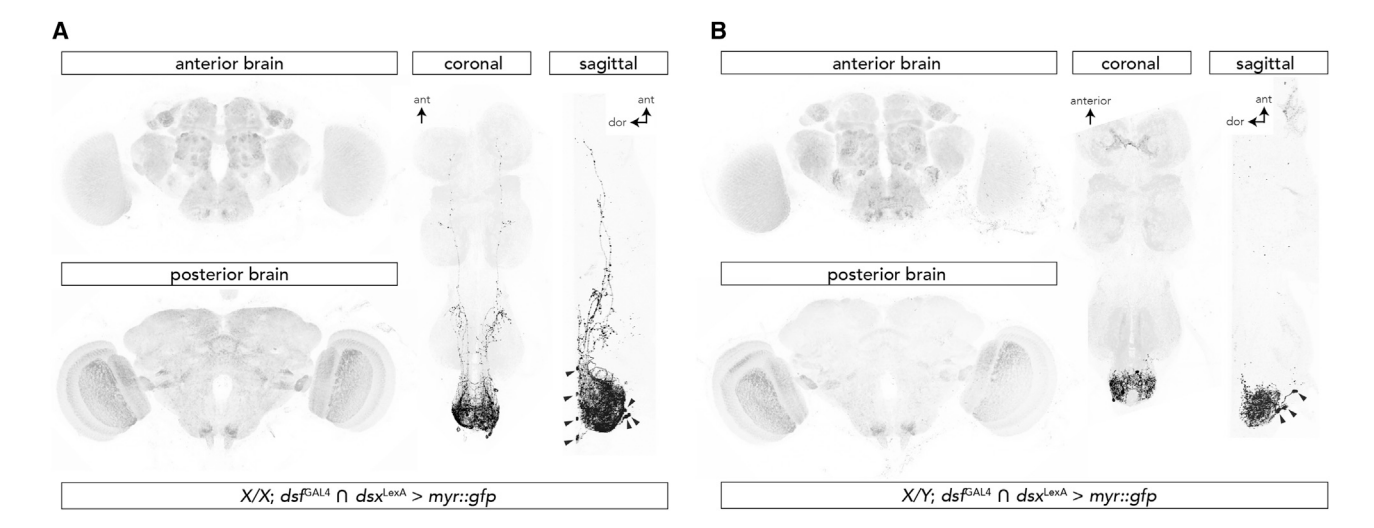


Figure 3. A sexually dimorphic group of dsf and dsx co-expressing interneurons in the abdominal ganglion (A and B) The intersection of dsf<sup>Gal4</sup> and dsx<sup>LexA</sup> targets the sexually dimorphic DDAG neurons in the abdominal ganglion of females (A) and males (B). GFPexpressing neurons and DNCad (neuropil) are shown in black and light gray, respectively.  $dsf^{Gal4} \cap dsx^{LexA}$  labels no other neurons in the VNC or brain. Arrowheads point to the cell bodies of the DDAG neurons. Not all cell bodies are visible.

suggest that the neuromuscular junction phenotypes of dsf mutant flies<sup>12</sup> may result from cell-non-autonomous actions of dsf. Taken together, we conclude that dsf is expressed in several subsets of neurons broadly distributed across the female and male CNS of adult, pupal, and larval stages and that Gal4 expression from the  $dsf^{Gal4}$  allele faithfully recapitulates the dsfwild-type expression pattern.

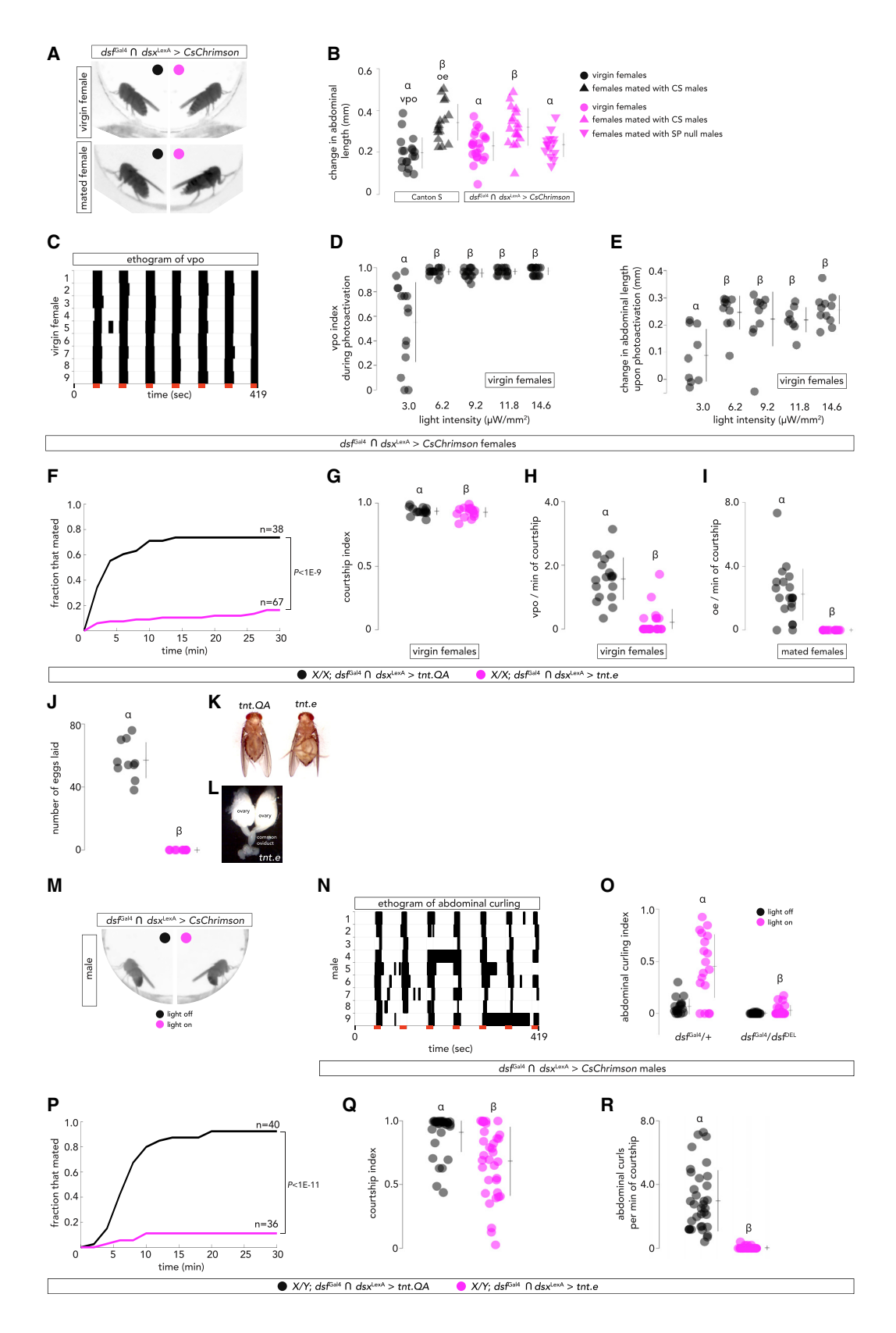
### A sexually dimorphic group of dsf and dsx co-expressing neurons contribute to female- and male-specific abdominal courtship behaviors

dsf contributes to courtship behaviors 12 that are also influenced by dsx gene function or dsx-expressing neurons. 6-8,20 We reasoned that dsf-expressing neurons relevant for courtship behaviors may co-express dsx. We therefore genetically intersected dsf<sup>Gal4</sup> with dsx<sup>LexA</sup>, <sup>20</sup> which expresses LexA::p65 in all dsx-expressing cells. dsx<sup>LexA</sup> was used to drive a LexAop-controlled Flp recombinase, which excised a transcriptional stop cassette from an upstream activating sequence (UAS)-myr::GFP transgene driven by dsf<sup>Gal4</sup>. This intersection (dsf<sup>Gal4</sup> ∩ dsx<sup>LexA</sup>) labeled a small group of sexually dimorphic interneurons (hereafter referred to as the DDAG neurons) in the abdominal ganglion of both sexes (Figures 3A and 3B). Males have three DDAG neurons on the left and right sides that arborize locally within the abdominal neuropil and whose cell bodies are located on the ventral side of the VNC. Females possess ∼11 DDAG interneurons, many of which are located on the dorsal side of the VNC. It is currently unclear whether females have homologs of the DDAG neurons found in males or whether females and males have entirely sex-specific DDAG neurons. The DDAG neurons of females arborize extensively within the abdominal ganglion, and some neurons extend neurites anteriorly to innervate all three thoracic neuropils. The intersection between dsf<sup>Gal4</sup> and dsx<sup>LexA</sup> did not appear to label any other cells in the brain or VNC (Figures 3A and 3B) nor any non-neuronal somatic tissues in the abdomen or elsewhere in the adult (data not shown).

To determine whether the DDAG neurons contribute to courtship behaviors, the  $dst^{Gal4} \cap dsx^{LexA}$  intersection was used to target the expression of the red light-gated cation channel CsChrimson<sup>21</sup> to activate the DDAG neurons. When stimulated with red light,  $dsf^{Gal4} \cap dsx^{LexA} > CsChrimson$  virgin females adjusted the posture and length of their abdomen and opened their vaginal plates, partially exposing their ovipositor (Figure 4A; Video S1). Virgin females normally open their vaginal plates if they are receptive to courting males<sup>22,23</sup> in contrast to mated females, which signal their unwillingness to mate by extruding their ovipositor. <sup>22,24,25</sup> The length of the female's abdomen increases during both behaviors, but by a greater amount during an ovipositor extrusion (Figure 4B). To confirm that photoactivation of the DDAG neurons in virgin females triggered an opening of the vaginal plates and not an ovipositor extrusion, we measured the change in abdomen length before and during photoactivation and compared it to the change in abdomen length when virgin females open their vaginal plates or when mated females extrude their ovipositor. Optogenetic activation of the DDAG neurons in virgin females induced a change in abdomen length more similar to that measured when virgin females open their vaginal plates during courtship than when mated females extrude their ovipositor (Figure 4B). Virgin dsf<sup>Gal4</sup> ∩ dsx<sup>LexA</sup> > CsChrimson females opened their vaginal plates immediately, and only during the photoactivation period (Figure 4C), and quantitatively similar behaviors were observed across a range of stimulus intensities (Figures 4D and 4E). In mated females, however, photoactivation of the DDAG neurons induced ovipositor extrusion (Figures 4A and 4B; Video S2), suggesting that female mating status alters the function of the DDAG neurons. Female receptivity in Drosophila is modified after mating by sex peptide (SP), a male seminal protein that is transferred to the female reproductive system during copulation.<sup>26</sup> When mated with SP null males,  $dsf^{Gal4} \cap dsx^{LexA} > CsChrimson$  females opened their vaginal plates instead of extruding their ovipositor during photoactivation (Figure 4B; Video S3). These data suggest that the DDAG







(legend on next page)

Please cite this article in press as: Duckhorn et al., Regulation of Drosophila courtship behavior by the TIx/tailless-like nuclear receptor, dissatisfaction, Current Biology (2022), https://doi.org/10.1016/j.cub.2022.02.031





neurons contribute to virgin or mated female abdominal behaviors depending on the mating status of the female.

We next tested whether the activity of the DDAG neurons is required for vaginal plate opening in virgin females and ovipositor extrusion in mated females. We used dsf<sup>Gal4</sup> ∩ dsx<sup>LexA</sup> to drive the expression of tetanus neurotoxin light chain (tnt.e)<sup>27</sup> to suppress the function of the DDAG neurons in virgin females. Compared to a control that expressed an inactive form of the neurotoxin (tnt.QA), virgin females that expressed tnt.e in the DDAG neurons mated infrequently with courting males (Figure 4F) despite being vigorously courted (Figure 4G) and exhibited a marked reduction in the frequency of vaginal plate opening during courtship (Figure 4H). Virgin females with inhibited DDAG neurons did not display behaviors indicative of mated females, such as ovipositor extrusion. Control females and females with inhibited DDAG neurons that eventually mated were tested 24 h later in courtship assays with wild-type males. Mated  $dsf^{Gal4} \cap dsx^{LexA} > tnt.e$  females extruded their ovipositor to courting males less frequently compared with mated tnt.QAexpressing control females (Figure 4I). Additionally, mated females with inhibited DDAG neurons produced and released eggs into the oviduct (Figure 4J) but failed to lay any eggs (Figure 4K) and eventually appeared gravid (Figure 4L). dsf null females lack synapses on the uterine wall<sup>12</sup> (Figures S2A-S2C), which correlates with their inability to lay eggs. However, inhibition of the DDAG neurons with tnt.e did not affect the presence or gross morphology of uterine synapses compared with tnt.QA-expressing control females (Figures S2D and S2E). A subset of DDAG neurons may thus contribute to egg laying by innervating uterine motoneurons. Together, these results demonstrate that activity of the DDAG neurons is required for vaginal plate opening in virgin females and ovipositor extrusion and later steps of egg laying in mated females.

In males, we observed that photoactivation of the DDAG neurons induced abdomen bending (Figures 4M-4O; Video S4). During Drosophila courtship, males attempt to copulate with females by curling their abdomen ventrally by  $\sim 180^{\circ}$  to achieve contact between genitalia. Males with inhibited DDAG neurons  $(dsf^{Gal4} \cap dsx^{LexA} > tnt.e)$  actively courted Canton S virgin females but were strongly reduced in successful mating rates relative to control ( $dsf^{Gal4} \cap dsx^{LexA} > tnt.QA$ ) males (Figures 4P and 4Q). Additionally, in comparison with controls, males with inhibited DDAG neurons showed markedly reduced frequency of abdomen bending per minute of active courtship (Figure 4R). We conclude that the DDAG neurons of females and males influence sex-specific abdominal behaviors during courtship.

### Sexually dimorphic anatomy and function of the DDAG neurons result from dsxM-mediated defeminization

We next sought to determine how the dimorphic development of the DDAG neurons is genetically regulated. dsf<sup>Gal4</sup> \(\cap{Gal4}\) dsx<sup>LexA</sup> > myr::gfp was used to visualize the DDAG neurons as before, but now we used a validated UAS-regulated short hairpin/miRNA (ShmiR) targeting dsx<sup>28,29</sup> to deplete male-specific dsx (dsxM) or female-specific dsx (dsxF) transcripts in dsfexpressing cells of both sexes. Depletion of male-specific dsx transcripts in dsf-expressing cells resulted in a near complete anatomical feminization of the DDAG neurons in males (compare Figure 5B with Figure 5A); males gained ~8 DDAG interneurons (Figure 5M) with an arborization pattern similar to that of the DDAG neurons of females (compare Figure 5B with Figure 5G). Knockdown of female-specific dsx transcripts, however, did

### Figure 4. Activity of the DDAG neurons is sufficient and necessary for female- and male-specific abdominal courtship behaviors

(A) A still-frame image of a  $dsf^{\text{Gal4}} \cap dsx^{\text{LexA}} > \text{CsChrimson}$  virgin and mated female, immobilized from decapitation, before (left) and during (right) illumination with 14.6 μW/mm<sup>2</sup> of red light to photoactivate the DDAG neurons. The virgin female opens her vaginal plates, whereas the mated female extrudes her ovipositor. See also Video S1.

- (B) The change in abdominal length upon an opening of the vaginal plates in virgin females and an ovipositor extrusion in mated females was measured and compared with the change in abdominal length induced upon photoactivation of the DDAG neurons in virgin females and females that mated with Canton S or sex peptide (SP) null males. See also Videos S2 and S3. vpo, vaginal plate opening; oe, ovipositor extrusion.
- (C) An ethogram of vaginal plate opening behavior of nine  $dsf^{Gal4} \cap dsx^{LexA} > CsChrimson$  virgin females during seven 15-s bouts of photoactivation (red bars). Black bars indicate when the female opens her vaginal plates.
- (D and E) Fraction of time a virgin female opens her vaginal plates during a 15 s bout of photoactivation (i.e., vpo index) and the change in abdominal length upon photoactivation are largely unchanged across a variety of light intensities.
- (F-I) Virgin females with inhibited DDAG neurons using tetanus neurotoxin (magenta) are unreceptive to active male courtship and exhibit a reduced frequency of vaginal plate opening behaviors relative to the control (black). (F) Fraction of virgin females that mated with a Canton S male over 30 min. (G) Fraction of time a Canton S male spent courting a virgin female during 5 min of observation (i.e., courtship index). Number of times a virgin female opened her vaginal plates (H) or a mated female extruded her ovipositor (I) per minute of active courtship by a Canton S male.
- (J) Number of eggs laid by a female 20-22 h after mating.
- (K) Mated females with inhibited DDAG neurons (tnt.e) appear gravid due to egg retention relative to control (tnt.QA) females.
- (L) Eggs are observed in the oviducts of a mated female with inhibited DDAG neurons, indicating that they ovulate. See also Figure S2.
- (M) A still-frame image of a decapitated dsf<sup>Gal4</sup> Ω dsx<sup>LexA</sup> > CsChrimson male before (left) and during (right) illumination with 14.6 μW/mm² of red light to photoactivate the DDAG neurons. Photoactivation results in abdominal curling without extrusion of the male's terminalia. See also Video S4
- (N) An ethogram of abdominal curling of nine dsf<sup>Gal4</sup> ∩ dsx<sup>LexA</sup> > CsChrimson males during seven 15-s bouts of photoactivation (red bars). Black bars indicate when the male curls his abdomen.
- (O) The fraction of time a dsf<sup>Gal4</sup> ∩ dsx<sup>LexA</sup> > CsChrimson male curls his abdomen (i.e., abdominal curling index) during bouts of photoactivation (magenta) and darkness (black) in a dsf heterozygous (dsf<sup>Gal4</sup>/+) and dsf mutant (dsf<sup>Gal4</sup>/dsf<sup>Del</sup>) background.
- (P-R) Males with inhibited DDAG neurons using tetanus neurotoxin (magenta) exhibit reduced mating rates and frequency of abdominal curls per minute of active courtship relative to the control (black). (P) Fraction of males that mated with a Canton S virgin female over 30 min. (Q) Fraction of time a male spent courting a virgin Canton S female during 5 min of observation. (R) Number of times a male curled his abdomen per minute of courtship. See also Figure S3.
- (B), (D), (E), (G)–(J), (O), (Q), and (R) show individual points, mean, and SD. Significance (p < 0.05) was measured in (B, D, and O) using a one-way ANOVA with a Tukey-Kramer test for multiple comparisons, in (G-J, Q, and R) using a Rank Sum test, and in (F and P) using a Logrank test. Same letter denotes no significant

### **Article**



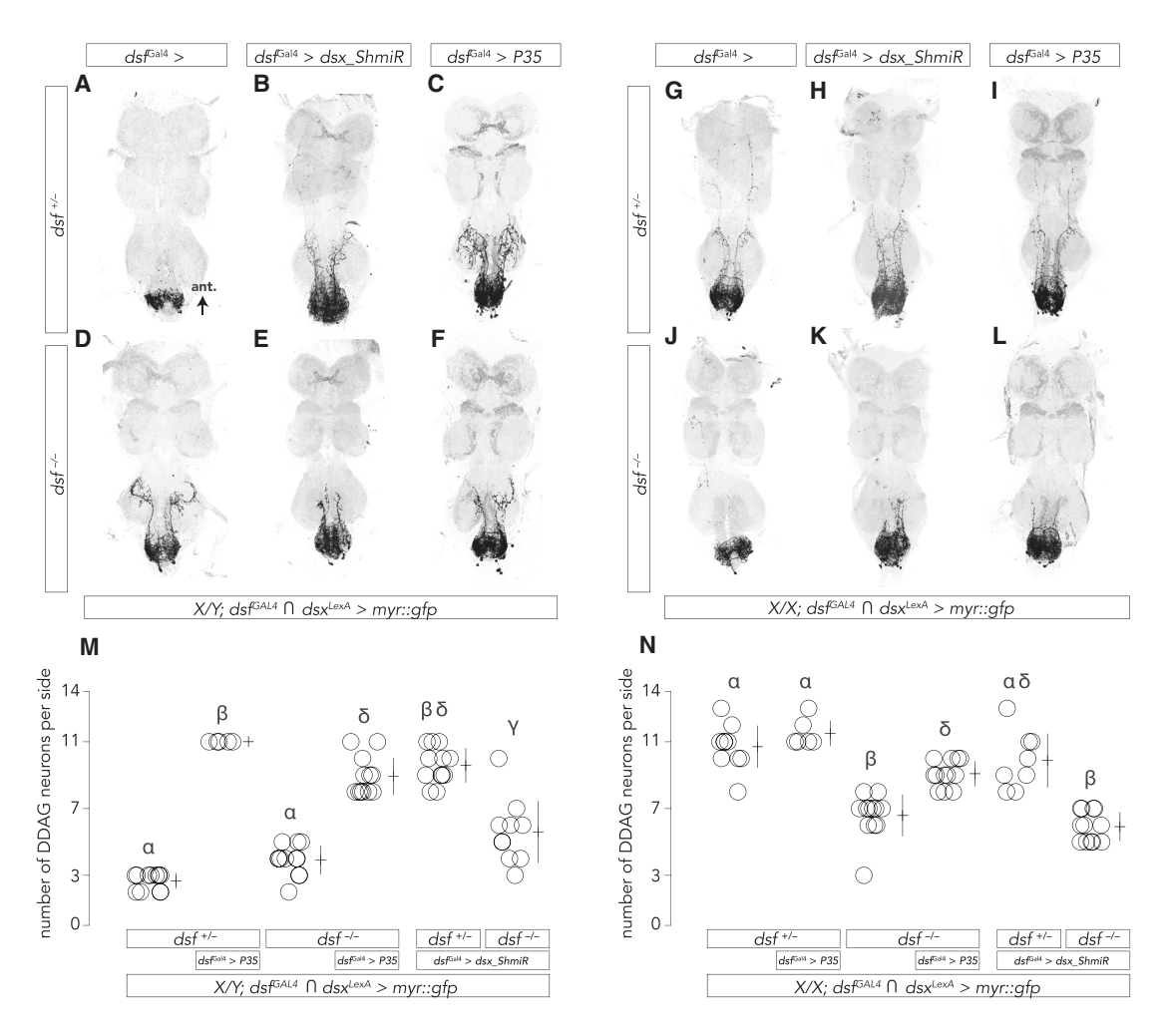


Figure 5. dsx and dsf influence sexually dimorphic DDAG neuron number through regulation of cell death

(A–L) Exemplary confocal images of male (A–F) and female (G–L) VNCs from the genotypes analyzed in (M) and (N), respectively. The DDAG neurons were visualized in dsf<sup>Gal4</sup> \(\tau\) dsx<sup>LexA</sup> > myr::gfp flies. GFP-expressing neurons and DNCad (neuropil) are shown in black and light gray, respectively.

(M and N) The number of DDAG neurons per side in the VNCs of males (M) and females (N). (M and N) Show individual points, mean, and SD. Significance (p < 0.05) was measured using a one-way ANOVA with a Tukey-Kramer test for multiple comparisons. Same letter denotes no significant difference.

not result in any obvious changes in DDAG neuron morphology or number (compare Figure 5H with Figure 5G; Figure 5N). These results indicate that sex differences in the DDAG neurons result at least in part from *dsx*M-mediated defeminization, whereby *dsx*M removes a set of neurons normally found in females. In the absence of sexual differentiation (i.e., without *dsx* function), the DDAG neurons develop the same in both sexes but in the likeness of DDAG neurons normally observed in females.

To test whether dsxM removes female-specific DDAG neurons by apoptosis, we used  $dsf^{\rm Gal4}$  to ectopically express the baculoviral caspase inhibitor, P35,  $^{30}$  in the DDAG neurons. Inhibition of cell death in males resulted in the gain of  $\sim$ 8 DDAG neurons (Figure 5M) that exhibited grossly female-like projection patterns (compare Figure 5C with Figure 5G). The morphology of the resurrected DDAG neurons in males is not fully feminized, however, most likely due to the expression of dsxM. Inhibition of cell death did not change the number of DDAG neurons in females (Figure 5N; compare Figure 5I with Figure 5G). These data demonstrate that dsxM is required for apoptosis of a subset of DDAG

neurons in males that otherwise survive in females due to the absence of *dsx*M activity.

To determine whether the depletion of dsx activity influences the function of the DDAG neurons, we photoactivated the DDAG neurons in females and males in which dsx\_ShmiR was driven by dsf<sup>Gal4</sup>. Photoactivation triggered the opening of the vaginal plates in females, similar to control females that lacked the UAS-dsx\_ShmiR transgene (Figure 6A; Video S5), consistent with the absence of an obvious neuroanatomical phenotype in the DDAG neurons of dsf<sup>Gal4</sup> > UAS-dsx\_ShmiR females. In contrast, photoactivation failed to induce abdomen curling in males but instead triggered a behavior in which the males extended their abdomen and extruded their terminalia (i.e., the terminal appendage consisting of genital and anal structures) during the illumination bout (Figures 6B and 6C; Video S6). Terminalia extrusion was never observed when the DDAG neurons were photoactivated in control males (Figure 6C; Video S4), suggesting that this behavior is gained in males with feminized DDAG neurons. Although courting males normally extrude their



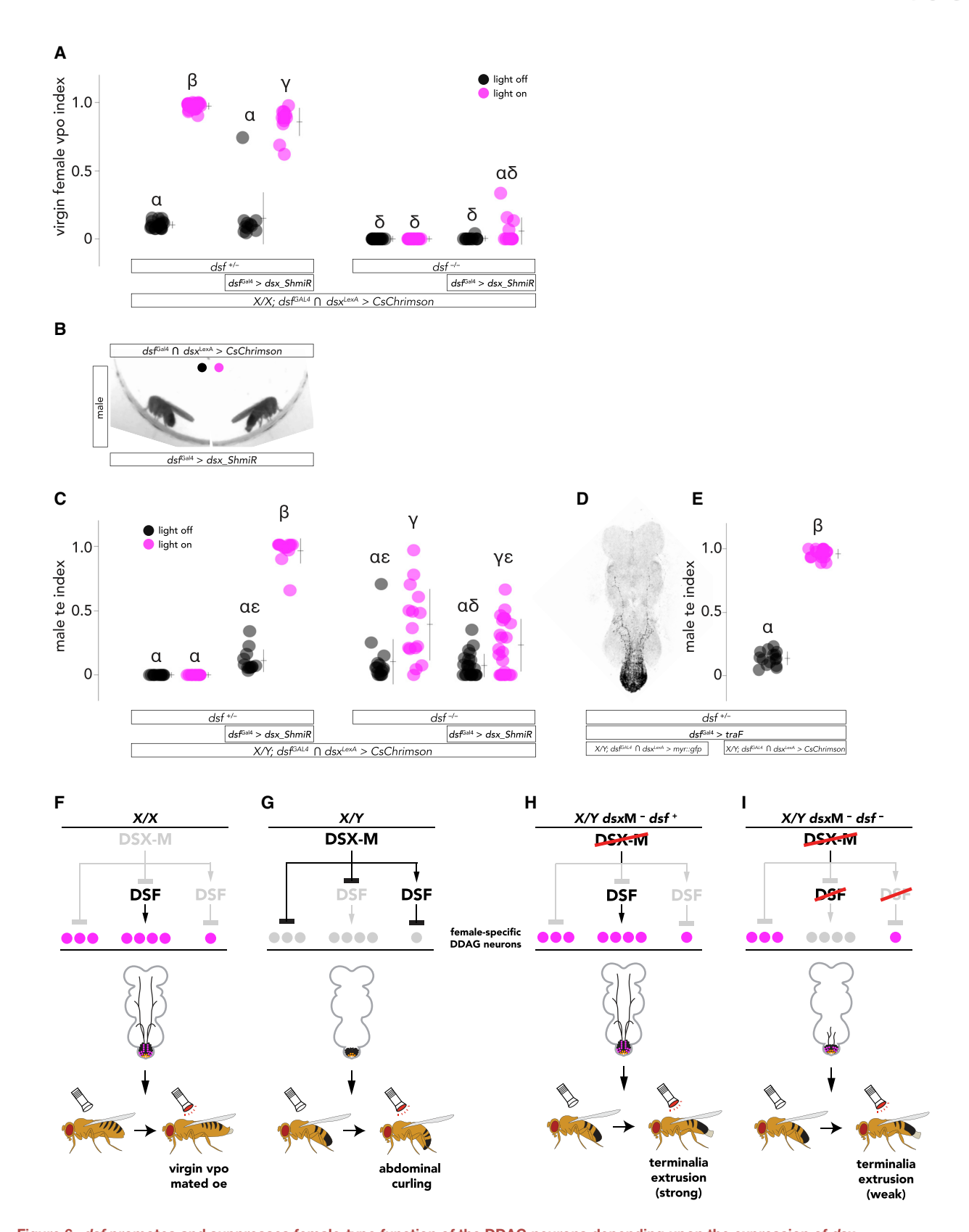


Figure 6. dsf promotes and suppresses female-type function of the DDAG neurons depending upon the expression of dsx (A) The fraction of time a virgin female expressing CsChrimson in the DDAG neurons spends with her vaginal plates open (i.e., vpo index) during darkness (black) and during 15 s bouts of photoactivation (magenta) with 14.6  $\mu$ W/mm<sup>2</sup> of red light. See also Videos S5 and S7.

Please cite this article in press as: Duckhorn et al., Regulation of Drosophila courtship behavior by the Tix/tailless-like nuclear receptor, dissatisfaction, Current Biology (2022), https://doi.org/10.1016/j.cub.2022.02.031

### **Current Biology**

### Article



terminalia as they curl their abdomen during a copulation attempt, the terminalia extrusions resulting from photoactivation of feminized DDAG neurons were accompanied by postural changes in the abdomen that phenocopy female-like abdominal courtship behaviors, such as vaginal plate opening or ovipositor extrusion (Figure 6B; Video S6).

To confirm that these artificially induced terminalia extrusions result from a feminization of the DDAG neurons, we constructed dsf<sup>Gal4</sup> ∩ dsx<sup>LexA</sup> > CsChrimson males that included a UASregulated female-specific transformer (traF) transgene<sup>31</sup> as an alternative strategy to feminize the DDAG neurons (Figure 6D). When stimulated with red light, the DDAG neurons of dsf<sup>Gal4</sup> > UAS-traF males triggered extrusions of the terminalia in ways and at levels similar to what was observed for dsf<sup>Gal4</sup> > UAS-dsx\_ShmiR males (Figure 6E).

We next sought to determine how depletion of dsx transcripts in the DDAG neurons may affect the courtship behaviors of females and males. Using dsfGal4 to drive the expression of dsx\_ShmiR, we found that a reduction of dsxF in the DDAG neurons of females did not affect mating rates with wild-type males (Figure S3A) nor the frequency of vaginal plate openings per minute of courtship (Figure S3B), but  $dsf^{Gal4} > dsx\_ShmiR$  females laid fewer eggs (Figure S3C) than control females. Depletion of dsxM transcripts in the DDAG neurons of males led to reduced mating rates with wild-type virgin females (Figure S3D) and reduced frequency of abdominal bends during courtship (Figure S3E). dsf<sup>Gal4</sup> > dsx\_ShmiR males were never observed to extrude their terminalia during courtship. Taken together, these results indicate that male-specific dsx defeminizes the anatomy and function of the DDAG neurons in part by directing the cell death of female-specific DDAG neurons that contribute to female-specific abdominal courtship behaviors.

### dsf exerts opposite effects on the development and function of the DDAG neurons in females and males, depending upon the expression of dsxM

Females carrying loss-of-function mutations in dsf mate infrequently with courting males, and dsf mutant males exhibit reduced copulation rates that correlate with abnormalities in abdomen bending during courtship. 12 Our results demonstrate that the DDAG neurons influence most courtship traits altered in dsf mutants. To determine whether dsf gene function is required specifically in the DDAG neurons for wild-type abdominal courtship behaviors, we depleted dsf expression in the DDAG neurons using  $dsx^{Gal4(\Delta 2)32}$  and a validated UAScontrolled dsf\_ShmiR. Compared with controls that carried only either the Gal4 or UAS transgenes,  $dsx^{Gal4(\Delta 2)} > dsf$  ShmiR virgin females mated infrequently with courting Canton S males, displayed a reduction in the frequency of vaginal plate opening during active male courtship, and retained their eggs (Figures S3F-S3H). Depletion of dsf transcripts in the DDAG neurons of males resulted in reduced mating rates with Canton S virgin females and a reduced frequency of abdomen bends during courtship (Figures S3I and S3J). These data suggest that dsf function is required in the DDAG neurons for female- and malespecific abdominal courtship behaviors that are altered in dsf mutants.

We next asked whether dsf influences the development of the DDAG neurons. We used  $dsf^{Gal4} \cap dsx^{LexA} > myr::gfp$  to visualize and compare the DDAG neurons of a dsf loss-of-function mutant (dsf<sup>Gal4</sup>/dsf<sup>Del</sup>) with a heterozygous control (dsf<sup>Gal4</sup>/+). Control females have ~11 bilaterally paired DDAG neurons on the left and right sides of the VNC, about four of which are lost in the absence of dsf function (Figure 5N). Additionally, the neurites of the DDAG neurons that normally project to the thoracic ganglia in control females were substantially reduced in dsf mutant females (compare Figure 5J with Figure 5G). dsf may influence DDAG neuron number by promoting the survival of a subset of DDAG neurons in females that would otherwise undergo apoptosis in the absence of dsf activity. Indeed, the number of DDAG neurons in dsf mutant females was partially restored when dsf<sup>Gal4</sup> was used to drive the expression of baculoviral P35 (Figure 5N; compare Figure 5L with Figure 5J). Similar results were observed in dsf mutant males (Figure 5M; compare Figure 5F with

In males, the loss of dsf resulted in a gain of a single bilateral pair of DDAG neurons in the dorsal abdominal ganglion (Figure 5M; compare Figure 5D with Figure 5A). This neuron extends a neurite shaped like a handlebar mustache anteriorly to innervate the third thoracic neuropil (Figure 5D). Both the neuron's location on the dorsal side and its gross projection pattern are similar to DDAG neurons found in females, suggesting that the loss of dsf activity in males may have partially feminized the DDAG neurons. To determine how the loss of dsf activity may affect the function of the DDAG neurons, we photoactivated the DDAG neurons in dsf mutant females and males  $(dsf^{Gal4}/dsf^{Del} \cap dsx^{LexA} > CsChrimson)$ . In contrast to control  $(dsf^{Gal4} \cap dsx^{LexA} > CsChrimson)$  females, photoactivation of the DDAG neurons in dsf mutants did not elicit vaginal plate opening (Figure 6A; Video S7) nor abdominal curling in males (Figure 50), but dsf mutant males extruded their terminalia during bouts of illumination (Figure 6C; Video S8). The fraction of

<sup>(</sup>B) A still-frame image of a decapitated dsf Gal4 > UAS-dsx\_ShmiR male before (left) and during (right) photoactivation of the DDAG neurons with 14.6 μW/mm² of red light performing a terminalia extrusion.

<sup>(</sup>C) The fraction of time a male expressing CsChrimson in the DDAG neurons spends extruding his terminalia (i.e., terminalia extrusion, or te, index) during darkness (black) and during 15 s bouts of photoactivation (magenta) with 14.6 µW/mm² of red light. See also Videos S6 and S8.

<sup>(</sup>D) An exemplary VNC from a traF-expressing male exhibiting fully feminized DDAG neurons.

<sup>(</sup>E) The te index of a traF-expressing male before (black) and during (magenta) photoactivation of the DDAG neurons with 14.6 µW/mm² of red light.

<sup>(</sup>F and G) Model for dsx and dsf function in regulating the number of female-specific DDAG neurons in wild-type females (F) and males (G) and the resulting neuroanatomical and behavioral outcomes. Female-specific DDAG neurons are shown in magenta. This model assumes that females share the DDAG neurons found in males, which are shown in orange.

<sup>(</sup>H and I) Loss of dsf activity in males with depleted dsxM expression is predicted to result in a loss of four female-specific DDAG neurons and reduced levels of terminalia extrusion upon photoactivation of the DDAG neurons.

<sup>(</sup>A, C, and E) Show individual points, mean, and SD. Significance (p < 0.05) was measured using a one-way ANOVA with a Tukey-Kramer post hoc test for multiple comparisons. Same letter denotes no significant difference.

Please cite this article in press as: Duckhorn et al., Regulation of *Drosophila* courtship behavior by the *Tlx/tailless*-like nuclear receptor, *dissatisfaction*, Current Biology (2022), https://doi.org/10.1016/j.cub.2022.02.031



# Current Biology

time *dsf* mutant males extruded their terminalia during an illumination bout was variable, and some *dsf* mutant males extruded their terminalia even after the illumination period had ended (Figure 6C). These results demonstrate that *dsf* promotes the presence of about 4 female-specific DDAG neurons in females, but functions in an opposite manner in males, suppressing the presence of a single female-like DDAG neuron whose activity is associated with a feminized abdominal behavior, i.e., terminalia extrusion.

These observations support a model where *dsf* regulates the development of the DDAG neurons depending upon expression of *dsx*M. In females, when *dsx*M is absent, *dsf* promotes the survival of four female-specific DDAG neurons that likely contribute to female-specific abdominal courtship behaviors (Figure 6F). In males, *dsx*M blocks *dsf* function in promoting the presence of these female-specific neurons (Figure 6G). *dsx*M defeminizes the DDAG neurons also by directly removing three female-specific neurons and by activating *dsf* s role in suppressing the presence of a single female-like DDAG neuron (Figure 6G). In this model, loss of *dsf* function in males with reduced *dsx*M expression is predicted to result in the loss of four female-like DDAG neurons and reduced levels of photoactivated terminalia extrusion behavior relative to males with only depleted *dsx*M transcripts (Figures 6H and 6I).

Indeed, removal of *dsf* function in males with reduced *dsx*M expression led to a loss of about four DDAG neurons and a reduction of anteriorly projecting neurites compared with control flies with only reduced *dsx*M expression (Figure 5M; compare Figure 5B with Figure 5E). Removal of *dsf* activity in females with or without *dsx*F activity caused a similar phenotype (Figure 5N; compare Figure 5G with Figure 5J and Figure 5H with Figure 5K). Additionally, males with reduced *dsx*M expression extruded their terminalia upon DDAG photoactivation at lower levels when *dsf* function was removed (Figure 6C). Photoactivation of the DDAG neurons in *dsf* mutant females did not induce vaginal plate opening behavior with or without depletion of *dsx*F expression (Figure 6A). These results suggest that *dsf* acts as both a "pro-female" and "anti-female" factor for DDAG development and function depending upon the expression of *dsx*M.

### **DISCUSSION**

We have discovered a sexually dimorphic group of dsf and dsx co-expressing abdominal interneurons called the DDAG neurons that contribute to vaginal plate opening in virgin females, ovipositor extrusion in mated females, and abdominal curling in males during courtship. We provide evidence that male-specific dsx directs the dimorphic development of the DDAG neurons in part through regulation of dsf activity. Depending upon the absence or presence of dsxM, dsf promotes the development of female-type DDAG neurons that regulate the opening of the vaginal plates in females but act in an opposite manner in males, suppressing the development of female-like DDAG neurons and abdominal behaviors. Several groups of dsf-expressing and dsx-non-expressing neurons in the brain also exhibit sex differences in cell number. These neurons likely co-express fru and may contribute to other sex-specific behaviors altered in dsf mutants.

Neural circuits for vaginal plate opening and ovipositor extrusion and their regulation by the female's mating status have been

elucidated recently. 22-24 We hypothesize that the DDAG neurons function as a conduit between the descending neurons, vpoDN and DNp13, and the motor circuits for vaginal plate opening and ovipositor extrusion, respectively. 23,24 We have shown that optogenetic activation of the DDAG neurons triggers vaginal plate opening or ovipositor extrusion depending upon the female's mating status. How the activity of the DDAG neurons is integrated with the female mating state is currently unclear. A recent study showed that ppk+ mechanosensory neurons in the female reproductive tract sense ovulation, and their activity permits the DNp13 neurons to engage the motor circuits for ovipositor extrusion.<sup>24</sup> One possibility is that vaginal plate opening and ovipositor extrusion are controlled by distinct subtypes of DDAG neurons. The DDAG subtypes that influence ovipositor extrusion may function downstream of the DNp13 neurons but upstream of the site at which ppk+ sensory neurons integrate with the neural circuit for ovipositor extrusion.

dsf encodes an orphan nuclear receptor homologous to the *Drosophila tailless* (*tll*) and vertebrate *Tlx* genes. <sup>13</sup> In mice, *Tlx* is expressed in all adult neural stem cells, <sup>33</sup> where it functions to maintain the cells in a proliferative state. <sup>34,35</sup> Similarly, in *Drosophila*, *tll* regulates the maintenance and proliferation of most neural progenitors in the protocerebrum. <sup>36</sup> At the developmental stages we examined, *dsf* <sup>Gal4</sup> expression in the VNC was observed exclusively in mature neurons and not in any neuronal progenitors. This suggest that *dsf* may regulate neuron number post-mitotically, directing the survival or apoptosis of female-specific DDAG neurons depending upon expression of *dsx*M.

The mechanism by which dsf function is altered by dsxM is currently unclear. Although nuclear receptors, including dsf, generally act as transcriptional repressors, some can also function as activators upon binding to a ligand 37-39 or after posttranslational modification. 40 Thus, in one scenario, the expression of DSX-M could sex-specifically impact DSF activity by regulating the generation of DSF's ligand (if it has one) or the occurrence of a post-translational modification. Alternatively (but not exclusively), expression of dsf may be directly regulated by DSX proteins. Consistent with this scenario, an in vivo genome-wide study of DSX occupancy identified dsf as a putative DSX target gene. 41 It is therefore possible that DSX-M sexspecifically regulates dsf expression in a subset of DDAG neurons that contribute to female-specific abdominal behaviors, thereby directing the removal of the neurons in males but not in females.

### **STAR**\*METHODS

Detailed methods are provided in the online version of this paper and include the following:

- KEY RESOURCES TABLE
- RESOURCE AVAILABILITY
  - Lead contact
  - Materials availability
  - O Data and code availability
- EXPERIMENTAL MODEL AND SUBJECT DETAILS
- METHOD DETAILS
  - Construction of dsf<sup>Gal4</sup> and dsf<sup>Del</sup> alleles
  - o in situ HCR and immunohistochemistry

### **Article**



- Behavior and optogenetic assays
- QUANTIFICATION AND STATISTICAL ANALYSIS

#### SUPPLEMENTAL INFORMATION

Supplemental information can be found online at https://doi.org/10.1016/j.cub.2022.02.031.

### **ACKNOWLEDGMENTS**

We thank Y. Ding, J. Lillvis, and E. Preger-Ben Noon for helpful discussions; A. McStravog for administrative assistance; and three reviewers for helpful comments on the manuscript. D.L.S. is an investigator with Howard Hughes Medical Institute. T.R.S. is supported by a grant from the National Science Foundation (IOS-1845673).

### **AUTHOR CONTRIBUTIONS**

Conceptualization, T.R.S., J.C.D., J.C., and D.L.S.; investigation, J.C.D., J.C., M.C.M., H.S., S.A., D.L.S., and T.R.S.; writing—original draft, T.R.S., D.L.S., and J.C.D.

### **DECLARATION OF INTERESTS**

The authors declare no competing interests.

Received: August 10, 2021 Revised: January 16, 2022 Accepted: February 9, 2022 Published: March 3, 2022

### REFERENCES

- Billeter, J.-C., Rideout, E.J., Dornan, A.J., and Goodwin, S.F. (2006). Control of male sexual behavior in *Drosophila* by the sex determination pathway. Curr. Biol. 16, R766–R776.
- Manoli, D.S., Foss, M., Villella, A., Taylor, B.J., Hall, J.C., and Baker, B.S. (2005). Male-specific fruitless specifies the neural substrates of *Drosophila* courtship behaviour. Nature 436, 395–400.
- 3. Demir, E., and Dickson, B.J. (2005). *fruitless* splicing specifies male courtship behavior in *Drosophila*. Cell *121*, 785–794.
- Stockinger, P., Kvitsiani, D., Rotkopf, S., Tirián, L., and Dickson, B.J. (2005). Neural circuitry that governs *Drosophila* male courtship behavior. Cell 121, 795–807.
- Robinett, C.C., Vaughan, A.G., Knapp, J.M., and Baker, B.S. (2010). Sex and the single cell. II. there is a time and place for sex. PLoS Biol. 8, e1000365.
- Rideout, E.J., Dornan, A.J., Neville, M.C., Eadie, S., and Goodwin, S.F. (2010). Control of sexual differentiation and behavior by the *doublesex* gene in *Drosophila melanogaster*. Nat. Neurosci. 13, 458–466.
- Waterbury, J.A., Jackson, L.L., and Schedl, P. (1999). Analysis of the doublesex female protein in *Drosophila melanogaster*: role in sexual differentiation and behavior and dependence on intersex. Genetics 152, 1653– 1667
- Shirangi, T.R., Taylor, B.J., and McKeown, M. (2006). A double-switch system regulates male courtship behavior in male and female *Drosophila* melanogaster. Nat. Genet. 38, 1435–1439.
- Kvitsiani, D., and Dickson, B.J. (2006). Shared neural circuitry for female and male sexual behaviours in *Drosophila*. Curr. Biol. 16, R355–R356.
- Shirangi, T.R., and McKeown, M. (2007). Sex in flies: what "body-mind" dichotomy? Dev. Biol. 306, 10–19.
- Villella, A., and Hall, J.C. (2008). Chapter 3. Neurogenetics of courtship and mating in *Drosophila*. Adv. Genet. 62, 67–184.

- Finley, K.D., Taylor, B.J., Milstein, M., and McKeown, M. (1997). dissatisfaction, a gene involved in sex-specific behavior and neural development of *Drosophila melanogaster*. Proc. Natl. Acad. Sci. USA 94, 913–918.
- Finley, K.D., Edeen, P.T., Foss, M., Gross, E., Ghbeish, N., Palmer, R.H., Taylor, B.J., and McKeown, M. (1998). dissatisfaction encodes a taillesslike nuclear receptor expressed in a subset of CNS neurons controlling *Drosophila* sexual behavior. Neuron 21, 1363–1374.
- Choi, H.M.T., Schwarzkopf, M., Fornace, M.E., Acharya, A., Artavanis, G., Stegmaier, J., Cunha, A., and Pierce, N.A. (2018). Third-generation in situ hybridization chain reaction: multiplexed, quantitative, sensitive, versatile, robust. Development 145, dev165753.
- Choi, H.M.T., Beck, V.A., and Pierce, N.A. (2014). Next-generation in situ hybridization chain reaction: higher gain, lower cost, greater durability. ACS Nano 8, 4284–4294.
- Choi, H.M.T., Chang, J.Y., Trinh, L.A., Padilla, J.E., Fraser, S.E., and Pierce, N.A. (2010). Programmable *in situ* amplification for multiplexed imaging of mRNA expression. Nat. Biotechnol. 28, 1208–1212.
- Duckhorn, J.C., Junker, I., Ding, Y., and Shirangi, T.R. (2021). Combined in situ hybridization chain reaction and immunostaining to visualize gene expression in whole-mount *Drosophila* central nervous systems. Preprint at bioRxiv. https://doi.org/10.1101/2021.08.09.455671.
- Court, R., Namiki, S., Armstrong, J.D., Börner, J., Card, G., Costa, M., Dickinson, M., Duch, C., Korff, W., Mann, R., et al. (2020). A systematic nomenclature for the *Drosophila* ventral nerve cord. Neuron 107, 1071– 1079 e2
- Ito, K., Shinomiya, K., Ito, M., Armstrong, J.D., Boyan, G., Hartenstein, V., Harzsch, S., Heisenberg, M., Homberg, U., Jenett, A., et al. (2014). A systematic nomenclature for the insect brain. Neuron 81, 755–765.
- Zhou, C., Pan, Y., Robinett, C.C., Meissner, G.W., and Baker, B.S. (2014).
   Central brain neurons expressing doublesex regulate female receptivity in Drosophila. Neuron 83, 149–163.
- Klapoetke, N.C., Murata, Y., Kim, S.S., Pulver, S.R., Birdsey-Benson, A., Cho, Y.K., Morimoto, T.K., Chuong, A.S., Carpenter, E.J., Tian, Z., et al. (2014). Independent optical excitation of distinct neural populations. Nat. Methods 11, 338–346.
- Mezzera, C., Brotas, M., Gaspar, M., Pavlou, H.J., Goodwin, S.F., and Vasconcelos, M.L. (2020). Ovipositor extrusion promotes the transition from courtship to copulation and signals female acceptance in *Drosophila melanogaster*. Curr. Biol. 30, 3736–3748.e5.
- Wang, K., Wang, F., Forknall, N., Yang, T., Patrick, C., Parekh, R., and Dickson, B.J. (2021). Neural circuit mechanisms of sexual receptivity in *Drosophila* females. Nature 589, 577–581.
- Wang, F., Wang, K., Forknall, N., Parekh, R., and Dickson, B.J. (2020).
   Circuit and behavioral mechanisms of sexual rejection by *Drosophila* females. Curr. Biol. 30, 3749–3760.e3.
- Kimura, K.I., Sato, C., Koganezawa, M., and Yamamoto, D. (2015). Drosophila ovipositor extension in mating behavior and egg deposition in-volves distinct sets of brain interneurons. PLoS One 10, e0126445.
- 26. Kubli, E. (1992). The sex-peptide. BioEssays 14, 779-784.
- Sweeney, S.T., Broadie, K., Keane, J., Niemann, H., and O'Kane, C.J. (1995). Targeted expression of tetanus toxin light chain in *Drosophila* specifically eliminates synaptic transmission and causes behavioral defects. Neuron 14, 341–351.
- Haley, B., Hendrix, D., Trang, V., and Levine, M. (2008). A simplified miRNA-based gene silencing method for *Drosophila melanogaster*. Dev. Biol. 321, 482–490.
- Shirangi, T.R., Wong, A.M., Truman, J.W., and Stern, D.L. (2016).
   Doublesex regulates the connectivity of a neural circuit controlling Drosophila male courtship song. Dev. Cell 37, 533–544.
- **30.** Hay, B.A., Wolff, T., and Rubin, G.M. (1994). Expression of baculovirus P35 prevents cell death in *Drosophila*. Development *120*, 2121–2129.
- McKeown, M., Belote, J.M., and Boggs, R.T. (1988). Ectopic expression of the female transformer gene product leads to female differentiation of chromosomally male *Drosophila*. Cell 53, 887–895.

Please cite this article in press as: Duckhorn et al., Regulation of Drosophila courtship behavior by the TIx/tailless-like nuclear receptor, dissatisfaction, Current Biology (2022), https://doi.org/10.1016/j.cub.2022.02.031



# **Current Biology**

- 32. Pan, Y.F., Robinett, C.C., and Baker, B.S. (2011). Turning males on: activation of male courtship behavior in Drosophila melanogaster. PLoS One
- 33. Shi, Y., Chichung Lie, D.C., Taupin, P., Nakashima, K., Ray, J., Yu, R.T., Gage, F.H., and Evans, R.M. (2004). Expression and function of orphan nuclear receptor TLX in adult neural stem cells. Nature 427, 78-83.
- 34. Liu, H.K., Belz, T., Bock, D., Takacs, A., Wu, H., Lichter, P., Chai, M., and Schütz, G. (2008). The nuclear receptor tailless is required for neurogenesis in the adult subventricular zone. Genes Dev. 22, 2473-2478.
- 35. Zhang, C.L., Zou, Y., He, W., Gage, F.H., and Evans, R.M. (2008). A role for adult TLX-positive neural stem cells in learning and behaviour. Nature 451, 1004-1007.
- 36. Younossi-Hartenstein, A., Green, P., Liaw, G.J., Rudolph, K., Lengyel, J., and Hartenstein, V. (1997). Control of early neurogenesis of the Drosophila brain by the head gap genes tll, otd, ems, and btd. Dev. Biol. 182, 270–283.
- 37. Mangelsdorf, D.J., and Evans, R.M. (1995). The RXR heterodimers and orphan receptors. Cell 83, 841-850.
- 38. Pitman, J.L., Tsai, C.C., Edeen, P.T., Finley, K.D., Evans, R.M., and McKeown, M. (2002). DSF nuclear receptor acts as a repressor in culture and in vivo. Dev. Biol. 245, 315-328.

- 39. Lee, J.W., Lee, Y.C., Na, S.Y., Jung, D.J., and Lee, S.K. (2001). Transcriptional coregulators of the nuclear receptor superfamily: coactivators and corepressors. Cell. Mol. Life Sci. 58, 289-297.
- 40. Hammer, G.D., Krylova, I., Zhang, Y., Darimont, B.D., Simpson, K., Weigel, N.L., and Ingraham, H.A. (1999). Phosphorylation of the nuclear receptor SF-1 modulates cofactor recruitment: integration of hormone signaling in reproduction and stress. Mol. Cell 3, 521-526.
- 41. Clough, E., Jimenez, E., Kim, Y.A., Whitworth, C., Neville, M.C., Hempel, L.U., Pavlou, H.J., Chen, Z.X., Sturgill, D., Dale, R.K., et al. (2014). Sexand tissue-specific functions of Drosophila doublesex transcription factor target genes. Dev. Cell 31, 761-773.
- 42. Port, F., Chen, H.M., Lee, T., and Bullock, S.L. (2014). Optimized CRISPR/ Cas tools for efficient germline and somatic genome engineering in Drosophila. Proc. Natl. Acad. Sci. USA 111, E2967-E2976.
- 43. Haley, B., Foys, B., and Levine, M. (2010). Vectors and parameters that enhance the efficacy of RNAi-mediated gene disruption in transgenic Drosophila. Proc. Natl. Acad. Sci. USA 107, 11435-11440.
- 44. Gibson, D.G., Young, L., Chuang, R.-Y., Venter, J.C., Hutchison, C.A., and Smith, H.O. (2009). Enzymatic assembly of DNA molecules up to several hundred kilobases. Nat. Methods 6, 343-345.

# **Current Biology Article**



### **STAR**\***METHODS**

### **KEY RESOURCES TABLE**

REAGENT or RESOURCE	SOURCE	IDENTIFIER
Antibodies		
abbit anti-GFP	Invitrogen	Cat#A11122; RRID:AB_221569
rat anti-DN-cadherin	Developmental Studies Hybridoma Bank	Cat#DN-Ex #8; RRID:AB_528121
mouse anti-Elav (9F8A9)	Developmental Studies Hybridoma Bank	Cat#Elav-9F8A9; RRID:AB_528217
goat anti-rat AlexaFluor 647	Invitrogen	Cat#A21247; RRID:AB_141778
Fluorescein (FITC)-conjugated donkey anti-rabbit	Jackson ImmunoResearch	Cat#711-095-152; RRID:AB_2315776
goat anti-mouse AlexaFluor 568	Invitrogen	Cat#A11004; RRID:AB_2534072
Chemicals, peptides, and recombinant proteins		
JitraPure 20X SSC Buffer	Invitrogen	Cat#15557044
/ectaShield	Vector Laboratories	Cat# H-1000; RRID:AB_2336789
DPX	Sigma-Aldrich	Cat#06522
all-trans-Retinal	Sigma-Aldrich	Cat#R2500
Critical commercial assays		
HCR RNA-FISH Bundle	Molecular Instruments	N/A
Experimental models: Organisms/strains		
Canton S		N/A
v <sup>1118</sup>		N/A
Df(2L)ED284/CyO	BDSC	RRID:BDSC_8040
Df(2L)BSC183/CyO	BDSC	RRID:BDSC_9611
DJFRC32-10XUAS-IVS-nlsGFP (attP40)	Janelia Research Campus (JRC), HHMI	N/A
JFRC29-10XUAS-IVS-myr::GFP-p10 (attP2)	JRC	N/A
dsx <sup>LexA::p65</sup> /TM6B	Zhou et al. <sup>20</sup>	N/A
oJFRC79-8XLexAop2-FlpL (attP40)	JRC, <sup>29</sup>	N/A
oJFRC41-10XUAS-FRT>STOP>FRT-myr::gfp su(Hw)attP1)	JRC, <sup>29</sup>	N/A
20XUAS-FRT>STOP>FRT-CsChrimson-mVenus (VK5)	JRC, <sup>29</sup>	N/A
JAS-FRT>STOP>FRT-tnt.e	B. Dickson <sup>29</sup>	N/A
JAS-FRT>STOP>FRT-tnt.QA	B. Dickson <sup>29</sup>	N/A
dsx <sup>Gal4(Δ2)</sup> /TM6B	Pan et al. <sup>32</sup>	N/A
P{y[+t7.7] v[+t1.8]=TRiP.GLV21010}attP2, e., UAS-dsx_ShmiR	Shirangi et al. <sup>29</sup>	RRID:BDSC_35645
JAS-traF	BDSC	RRID:BDSC_4590
JAS-P35 <sup>BH1</sup>	BDSC	RRID:BDSC_5072
1130/TM3	M. Wolfner (Cornell)	N/A
0325/TM3	M. Wolfner (Cornell)	N/A
JAS-dsf_ShmiR (attP2)	This study	N/A
Dligonucleotides		
Orosophila dsf HCR v3.0 probe set (B1)	Molecular Instruments	Lot # PRF061
31 488 HCR Amplifier	Molecular Instruments	N/A
Recombinant DNA		
BPGuW	Addgene	Addgene Plasmid #17575
pCFD4-U6:1_U6:3tandemgRNAs	Port et al. <sup>42</sup>	Addgene Plasmid #49411
Software and algorithms		
	NIH, USA	https://imagej.net/fiji
MATLAB	Mathworks	https://www.mathworks.com/products/

Please cite this article in press as: Duckhorn et al., Regulation of *Drosophila* courtship behavior by the *Tlx/tailless*-like nuclear receptor, *dissatisfaction*, Current Biology (2022), https://doi.org/10.1016/j.cub.2022.02.031





### **RESOURCE AVAILABILITY**

#### **Lead contact**

Further information and requests for resources and reagents should be directed to and will be fulfilled by the lead contact, Troy Shirangi (troy.shirangi@villanova.edu).

### **Materials availability**

Fly lines generated in this study are available from the lead contact.

### Data and code availability

All data reported in this paper will be shared by the lead contact upon request. This paper does not report original code. Any additional information required to reanalyze the data reported in this paper is available from the lead contact upon request.

### **EXPERIMENTAL MODEL AND SUBJECT DETAILS**

Drosophila melanogaster stocks were maintained on standard cornmeal and molasses food at 25°C and  $\sim$ 50% humidity in a 12-hr light/dark cycle unless otherwise noted. Fly stocks used in this study are listed in the key resources table. Sex Peptide null (SP<sup>0</sup>) males were generated by crossing  $\Delta 130/TM3$  males to 0325/TM3 females (gift from M. Wolfner, Cornell). UAS-dsf\_ShmiR (attP2) was created according to protocols described in Haley et al. Two stem-loops targeting sequences in dsf's fourth exon were placed into an intron from the ftz gene upstream of a cDNA encoding nls::gfp. This construct was cloned into the BglII/Xbal sites in pMUH.

### **METHOD DETAILS**

### Construction of dsf<sup>Gal4</sup> and dsf<sup>Del</sup> alleles

The *dsf*<sup>Gal4</sup> allele was created using CRISPR/Cas9-mediated homology-directed repair to precisely introduce Gal4 into *dsf*'s start codon in exon 1. The Gal4 cDNA/hsp70 yeast terminator sequence was amplified from pBPGuW (Addgene Plasmid #17575). A donor plasmid was generated by combining a 1,050-bp left homology arm, the Gal4/terminator sequence, 3XP3::DsRed marker (with an inverted orientation), a 1,149-bp right homology arm, and a 1.8-kb backbone using Gibson Assembly. <sup>44</sup> Guide RNAs (5'-CATCAACGGAAAATGGGCAC-3' and 5'-ATACTTCCATCAACGGAAAA-3') were cloned into the pCFD4 plasmid. <sup>42</sup> The donor and pCFD4 plasmids, *in vitro* transcribed codon optimized Cas9 mRNA, and a lig4 siRNA were co-injected into w<sup>1118</sup> embryos. The *dsf*<sup>Del</sup> allele was created using an identical strategy except the Gal4/terminator sequence was excluded from the donor plasmid.

### in situ HCR and immunohistochemistry

Nervous systems were dissected in 1X PBS, fixed in 4% paraformaldehyde buffered in PBS for 35 min at room temperature, and rinsed and washed in PBT (PBS with 1% Triton X-100), in situ hybridization chain reaction experiments were conducted as described <sup>17</sup> using HCR probe-sets (dsf-B1, Lot # PRF061) and hairpins (B1 488 HCR Amplifier) synthesized by Molecular Instruments™. We used a probe-set size of 20. After dissection and fixation, the tissues were pre-hybridized in prewarmed Probe Hybridization Buffer (Molecular Instruments™) for 30 minutes at 37°C and incubated with HCR probes in Probe Hybridization Buffer overnight at 37°C. Tissues were washed the next day in prewarmed Probe Wash Buffer four times, 15 minutes each at 37°C, and washed in 5X SSCT (UltraPure 20X SSC Buffer, Invitrogen #15557044, diluted in water) three times, 5 minutes at room temperature. Tissues were pre-amplified in Amplification Buffer (Molecular Instruments<sup>TM</sup>) for 30 minutes at room temperature and incubated with snap-cooled HCR hairpins in Amplification Buffer overnight at room temperature, protected from light. Tissues were then washed with 5X SSCT at room temperature twice for 5 minutes, twice for 30 minutes, and once for 5 minutes before being mounted in VectaShield (Vector Laboratories #H-1000) or proceeding with an immunohistochemistry protocol. Immunohistochemistry was performed as described.<sup>29</sup> Nervous systems were incubated with primary antibodies in PBT overnight at 4°C. Tissues were washed in PBT at room temperature for several hours and incubated overnight with secondary antibodies at 4°C. Tissues were washed in PBT for several hours at room temperature, mounted onto poly-lysine coated coverslips, dehydrated through an ethanol series, cleared in xylenes, and mounted in DPX (Sigma-Aldrich #06522) on a slide. If immunohistochemistry followed in situ HCR, nervous systems were mounted in Vectashield. The following antibodies were used: rabbit anti-GFP (Invitrogen #A11122; 1:1,000), rat anti-DN-cadherin (DN-Ex #8, Developmental Studies Hybridoma Bank; 1:50), mouse anti-Elav (9F8A9, Developmental Studies Hybridoma Bank; 1:20), AF-647 goat anti-rat (Invitrogen #A21247; 1:500), Fluorescein (FITC)-conjugated donkey anti-rabbit (Jackson ImmunoResearch #711-095-152; 1:500), AF-568 goat anti-mouse (Invitrogen #A11004; 1:500). Tissues were imaged on a Leica SP8 confocal microscope at 40X with optical sections at 0.3 μm intervals.

### **Behavior and optogenetic assays**

Newly eclosed flies were collected under  $CO_2$  anesthesia and aged for 7–10 days at 25°C and  $\sim$ 50% humidity in a 12-hr light/dark cycle unless otherwise noted. Virgin females and males used in optogenetic assays were raised in darkness at 25°C on food containing 0.2 mM all-*trans*-Retinal (Sigma-Aldrich #R2500) before and after eclosion, grouped in vials according to sex, and aged for 10–14 days. Flies were chilled on ice and decapitated under a low intensity of blue light (470 nm) and allowed to recover for

Please cite this article in press as: Duckhorn et al., Regulation of Drosophila courtship behavior by the Tix/tailless-like nuclear receptor, dissatisfaction, Current Biology (2022), https://doi.org/10.1016/j.cub.2022.02.031

### **Current Biology**

Article



~30 min before being transferred into behavioral chambers (diameter: 10 mm, height: 3 mm). The chambers were kept in darkness and placed above an LED panel that provided infrared light (850 nm) for continuous illumination and photoactivation with red light (635 nm). The intensity and pattern of red-light illumination were controlled by a customized Arduino script. Light intensity was confirmed with an optical power meter (Thorlabs, PM160). A camera (FLIR Blackfly S USB3, BFS-U3-31S4M-C) equipped with a long-pass filter (cut-on wavelength of 800 nm; Thorlabs, FEL0800) was placed above the chamber and videos were recorded at 55 fps with a resolution of 0.03 mm/pixel. Courtship and receptivity assays were conducted using group- and singly-housed virgin females and males, respectively. Behavior assays were done at  $25^{\circ}$ C under white light,  $\sim$ 1–2 hrs after the start of the subjective day. Individual females and naive males were loaded into behavioral chambers (diameter: 10 mm, height: 3 mm) and recorded for 30 min using a Sony Vixia HFR700 video camera. Ovipositor extrusion was assessed using mated females prepared 24 hrs before the assay by grouping 10 virgin females and 20 wild-type Canton S or SP<sup>0</sup> in a vial. Mated females were anesthetized on ice and sorted 30 min before the assay. Individual females and naive Canton S males were loaded into behavioral chambers as described above and video recorded for 15 min. For male abdominal curling measurements, virgin Canton S females and experimental or control males were collected and housed as described above. Virgin females were anesthetized on ice and decapitated to prevent copulation 30 min before being transferred individually into behavioral chambers with a male. The pairs were recorded for 15 min. Change in abdominal length was measured in ImageJ using frames before and during vaginal plate opening or ovipositor extrusion in which the female was in the same position in the chamber. A ruler was included in the video and used to set the scale of measurement in mm. The length of abdomen was measured by drawing a line from the base of scutellum to the posterior tip of the female's abdomen before and during vaginal plate opening or ovipositor extrusion. The change in abdominal length was determined by calculating the difference between the two measurements. The vaginal plate opening and abdominal curling indices were calculated by dividing the amount of time the female opened her vaginal plates or the male curled his abdomen by the total photoactivation time of each bout. Courtship index was measured as the total amount of time the male spent performing any courtship behavior divided by the total observation time.

### **QUANTIFICATION AND STATISTICAL ANALYSIS**

Data were analyzed using one-way ANOVA with Tukey-Kramer tests for multiple comparisons, Rank Sum tests, or Logrank tests. All p-values were measured in MATLAB.